

A Bayesian Nonparametric Approach to Dynamical Noise Reduction

Konstantinos Kaloudis, Spyridon J. Hatjispyros ¹

Department of Mathematics, Division of Statistics and Actuarial Science, University of the Aegean
Karlovassi, Samos, GR-832 00, Greece.

Abstract

We propose a Bayesian *nonparametric* approach for the noise reduction of a given chaotic time series contaminated by dynamical noise, based on Markov Chain Monte Carlo methods (MCMC). The underlying unknown noise process (possibly) exhibits heavy tailed behavior. We introduce the Dynamic Noise Reduction Replicator (DNRR) model with which we reconstruct the unknown dynamic equations and in parallel we replicate the dynamics under reduced noise level dynamical perturbations. The dynamic noise reduction procedure is demonstrated specifically in the case of polynomial maps. Simulations based on synthetic time series are presented.

Keywords: Bayesian nonparametric inference; Chaotic dynamical systems; Noise reduction; Random dynamical systems

1 Introduction

For over three decades, nonlinear dynamical systems [24] have been in the center of attention of a wide variety of sciences, giving the opportunity to model multiple time varying phenomena, exhibiting complex and irregular characteristics. The unpredictable nature of chaotic dynamics was early connected to probabilistic and statistical methods of analysis [1, 2]. Furthermore, the ubiquitous effect of different kinds of noise in experimental or real data reinforced the interaction between nonlinear dynamics and statistics [22]. In this context, noise reduction methods kept drawing the attention of the researchers from both a theoretical and an applied point of view.

Many different approaches have been adopted to address the issue of nonlinear noise reduction. Hammel et al. [11], used techniques originated from the proof of the shadowing lemma to reduce noise in observed chaotic data. Farmer and Sidorowich [7], proposed the use of Lagrangian multipliers for the minimization of the distance between the observed and the denoised orbit. In order to deal with homoclinic tangencies, they used a combination of manifold decomposition and singular value decomposition techniques. Locally linear models were introduced by Schreiber and Grassberger [28] for noise reduction, while Davies proposed initially gradient

¹Corresponding author. Tel.: +30 22730 82326

E-mail address: schatz@aegean.gr

descent [4] and later Levenberg-Marquardt [5] methods for the minimization of the dynamic error. The first attempt to a Bayesian noise reduction framework [26] was due to Davies [3]. Other methods include the usage of shadowing methods [18], wavelet transformations [17], Sequential Markov Chain methods [6] in the case of state space models, and Kalman filtering techniques [30], while important theoretical results about the consistency of signal extraction, under measurement noise, were presented by Lalley et al. [20, 21].

The type of noise contaminating the data is very important, because of the different effects induced by it. Observational or measurement noise, originating from errors in the measurement process, is independent of the dynamics and can be thought of as being added after the time evolution of the trajectories under consideration. On the other hand, dynamical or interactive noise, is added at each step of the time evolution of the trajectories, drastically modifying the underlying dynamics. Extensive studies on the effect of dynamical noise on the underlying deterministic system include the works of Jaeger and Kantz [16], and, Strumic and Macek [29]. Dynamical noise can represent the error in the assumed model, thus compensating for a small number of degrees of freedom, for example a small amplitude high dimensional deterministic part not included in the model [19]. Moreover, in the presence of dynamical noise, shadowing trajectories of non-hyperbolic maps is not possible. This problem was addressed by Kantz [15], introducing a noise reduction method based on “parameter shadowing”. In this work, a shadowing pseudo-orbit is generated, evolving in some neighborhood of the original orbit, fulfilling the nearby rather than the exact dynamics.

This work regards a fully Bayesian nonparametric method for the reduction of the additive dynamical noise perturbing an observed noisy time series (x_i) of length n . We develop the DNRR model, whereby we introduce the n strategic hidden random variables (Y_i) . Their posterior distribution describes all possible noise reduced trajectories in the neighborhood of the original trajectory, and we show that with the appropriate point estimation, we can recover a noise reduced trajectory (y_i) that for moderate noise levels is being generated by approximately the same dynamical system, generating the observed noisy time series, yet perturbed by a weaker error process. We also show that near the homoclinic tangencies of the associated deterministic system, the posterior marginal distributions Y_i become multimodal limiting the noise reduction levels.

The novelty of our approach lies on the fact that we make no parametric assumptions for the density of the noise component. Instead, we model the additive error using a highly flexible family of density functions, which are based on a Bayesian nonparametric model, namely the Geometric Stick Breaking process [8], extending previous works regarding reconstruction and prediction of random dynamical systems [13, 14, 23]. No matter what additive errors are involved, we are confident that our family of densities will be able to capture the right shape and hence statistical inference, for the parameters of interest will be improved and reliable. Under this formulation, the noise reduction method proposed can be applied to cases where the noise is not assumed to be normally distributed, or even in cases where we know that the

noise component has a mixture density. Such cases include, among others, scenarios where the noise is the result of multiple sources affecting the time evolution of the underlying dynamics. In this case, our method will be able to estimate the true noise density and moreover identify the number of the sources as the ergodic average of the active clusters.

The paper is organized as follows. In Sec. II we mention some aspects of the problem and present the noise reduction algorithm steps. In Sec. III we present the MCMC procedure for the estimation of the noise-reduced orbit. In Sec. IV we resort to simulation. We illustrate our method in the case of the random full quadratic and polynomial maps under non-Gaussian dynamical noise. We conclude in Sec. V giving some directions for further research.

2 Preliminaries

We define the random recurrence relation given by

$$\begin{aligned} X_i &= T(\theta, X_{i-1}, \dots, X_{i-d}, e_i) \\ &= g(\theta, X_{i-1}, \dots, X_{i-d}) + e_i, \quad i \geq 1, \end{aligned} \tag{1}$$

where $g : \Theta \times X^d \rightarrow X$, for some compact subset X of \mathbb{R} , $(X_i)_{i \geq -d+1}$ and $(e_i)_{i \geq 1}$ are real random variables over some probability space (Ω, \mathcal{F}, P) ; we denote by $\theta \in \Theta \subseteq \mathbb{R}^m$ any dependence of the deterministic map g on parameters. g is nonlinear, and for simplicity, continuous in $X_{i:d} := (X_{i-1}, \dots, X_{i-d})$. We assume that the random variables e_i are independent to each other, and independent of the states X_{i-r} for $r < i+d$. In addition we assume that the additive perturbations e_i are identically distributed from a zero mean distribution with unknown density f defined over the real line, so that $T : \Theta \times X^d \times \mathbb{R} \rightarrow \mathbb{R}$. Finally, notice that the lag-one stochastic process (W_i^1, \dots, W_i^d) , formed out, from time-delayed values of the (X_i) process, defined by

$$W_i^k = \begin{cases} g(\theta, W_{i-1}^1, \dots, W_{i-1}^d) + e_i & k = 1 \\ W_{i-1}^{k-1} & 1 < k \leq d, \end{cases}$$

is Markovian over \mathbb{R}^d .

We assume that there is no observational noise, so that we have at our disposal a time series $x^n := (x_1, \dots, x_n)$ generated by the nonlinear stochastic process defined in (1). The time series x^n depends solely on the initial distribution of $X_{1:d}$, the vector of parameters θ , and the particular realization of the noise process.

Orbits contaminated with dynamical noise are a -pseudo-orbits of the underlying g -dynamics in the sense that for all $1 \leq i \leq n$ there is positive a for which $0 < |x_i - g(\theta, x_{i:d})| \leq a$. g -invariant measures $\mu_g(dx)$ are deformed and smoothed-out into T -quasi-invariant measures $\mu_T(dx) = \lim_{t \rightarrow \infty} P\{x < X_t \leq x + dx | \tau_{X'} > t\}$, where $\tau_{X'}$ is a random time denoting the first passage time of the system to the unbounded trapping set $X' = \mathbb{R} \setminus X$. Mind that, μ_T is not a convolution of the unperturbed measure μ_g with the noise distribution, as it happens in the case of observational noise.

As a distance between the two time series x^n and y^n , we will use the average correction $E_0(x^n, y^n) = \sqrt{\frac{1}{n} \sum_{i=1}^n (x_i - y_i)^2}$. We will measure the overall deviation of the noisy orbit x^n from the g -determinism, with the average dynamical error $E_{\text{dyn}}(x^n; g) = \sqrt{\frac{1}{n} \sum_{i=1}^n (x_i - g(\theta, x_{i:d}))^2}$.

2.1 Dynamical noise reduction

Dynamical noise has a severe effect on the underlying dynamics, i.e. the deterministic part of the noisy corrupted time series, especially when the system under consideration is non-hyperbolic. In the hyperbolic case, the shadowing lemma guarantees the existence of shadowing pseudo-orbits and moreover if the dynamical noise is bounded, it can be treated as measurement noise. This means that we can find a g -deterministic orbit y^n and a noise process (\tilde{z}_i) such that $x_i = y_i + \tilde{z}_i$. The \tilde{z}_i errors are describing the distribution of the distance between the two orbits, and the x^n -dynamical noise reduction problem can be treated as a y^n -observational noise reduction problem. This is not valid, though, when the underlying dynamics are non-hyperbolic.

In the non-hyperbolic case, the presence of homoclinic tangencies (HTs) in the phase space, points where the stable and unstable manifold of a hyperbolic orbit intersect tangentially, is responsible for the emergence of a much more complicated structure. In the vicinity of HT's, the dynamic perturbations are amplifying dynamics away from the neighborhood of the attractor. One of the effects caused by the noise amplifications due to HT's are noise-induced prolongations [15]. For example, in Figure 1, we display the delay plots of the deterministic and a dynamically perturbed realization of the Hénon map of lengths $n = 5000$. The noisy trajectory, has been generated via

$$x_i = g(x_{i-1}, x_{i-2}) = 1.38 - x_{i-1}^2 + 0.27x_{i-2} + e_i, \quad (2)$$

where $e_i \stackrel{\text{i.i.d.}}{\sim} 0.6\mathcal{N}(0, \sigma^2) + 0.4\mathcal{N}(0, 100\sigma^2)$, for $\sigma^2 = 0.21 \times 10^{-4}$, with initial condition $x_0 = x_{-1} = 0.5$. The time series realization has been chosen, such that, the noise level is approximately 3%. We can see the intense noise induced prolongations, as clouds of points in red, away from the neighborhood of the deterministic attractor (points in black).

The deformation of the g -invariant measure to a T -quasi-invariant measure, leads to the expansion of its support, and the perturbed map visits areas of the phase space that was not able to visit without the effect of the dynamical noise.

We aim to reconstruct the underlying deterministic dynamics in the form of a map \hat{g}_{x^n} , and sample a y^n trajectory, such that we will be able to control its average deviation from determinacy $E_{\text{dyn}}(y^n, \hat{g}_{x^n})$, with respect to \hat{g}_{x^n} , as well as its average correction $E_0(x^n, y^n)$, with respect to x^n .

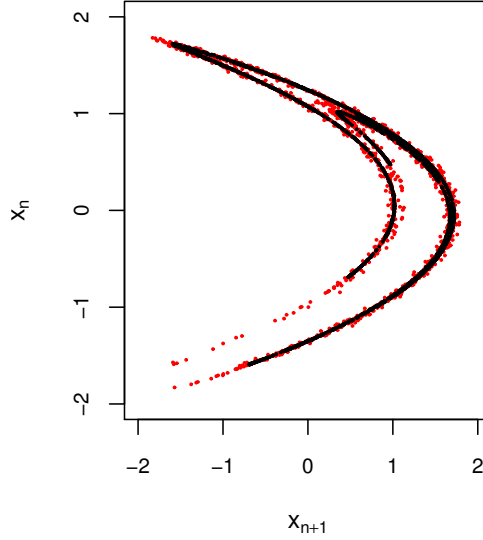


Figure 1: Noisy and deterministic Hénon trajectories, of length $n = 5000$, are depicted in red and black, respectively, for a 3% dynamical noise level.

2.2 Gaussian and non-Gaussian noise processes

We assume that the corrupting noise f , responsible for the observed time series x^n , can be represented as a countable mixture of zero mean normals $\mathcal{N}(z|0, \sigma_i^2)$ of variances σ_i^2 , that is

$$f(z) := f_M(z) = \sum_{i=1}^M p_i \mathcal{N}(z|0, \sigma_i^2)$$

with $p_i > 0$ and $\sum_{i=1}^M p_i = 1$, where M can be infinite. Then, the variance associated with f_M (when it exists), is the p_i -mixture of the σ_i^2 -variances i.e. $\sigma_{f_M}^2 = \sum_{i=1}^M p_i \sigma_i^2$. Following Jaeger and Kantz [15] we define the noise level η as the percentage of the sampling standard deviation of x^n (the signal), that is, $\eta = 100 \sigma_f / \sigma_{x^n}$.

As a measure of the departure from normality of the noise process f , we use the mean absolute deviation from the mean, normalized by the standard deviation. So for a zero mean $Z \sim f$ it is that $TF_f := \mathbb{E}|Z| / \sqrt{\mathbb{E}|Z|^2}$. The closer the quantity TF_f is to one, the thinner the tails are. We have the following lemma:

Lemma 1. *For all $M \geq 1$, it is that*

$$TF_{f_M} \leq TF_{f_1} \quad \text{with} \quad TF_{f_M} = \frac{1}{\sigma_{f_M}} \sqrt{\frac{2}{\pi}} \sum_{i=1}^M p_i \sigma_i. \quad (3)$$

Proof: We let $|Z| \sim f_+$, then it is clear that

$$f_+(z) = \frac{f_M(z) \mathcal{I}(z > 0)}{\int_{\mathbb{R}^+} f_M(z) dz} = 2 \sum_{i=1}^M p_i \mathcal{N}(z|0, \sigma_i^2) \mathcal{I}(z > 0),$$

where $\mathcal{I}(z > 0)$ is the characteristic function of the interval $(0, \infty)$. The equation for TF_{f_M} in (3) can be verified by the fact that $\int_{\mathbb{R}^+} z \mathcal{N}(z|0, \sigma_i^2) dz = \sigma_i \sqrt{2/\pi}$. By Jensen's concave inequality we have that $\sum_{i=1}^M p_i \sigma_i \leq \sigma_{f_M}$ or equivalently that $TF_{f_M} \leq TF_{f_1}$. \square

We consider the noise processes f_1 and $\{f_{2,l} : 1 \leq l \leq 4\}$ given by

$$\begin{aligned} f_1(z) &= \mathcal{N}(z|0, \sigma^2) \\ f_{2,l}(z) &= \frac{5+l}{10} \mathcal{N}(z|0, \sigma^2) + \frac{5-l}{10} \mathcal{N}(z|0, 100\sigma^2). \end{aligned} \tag{4}$$

From lemma 1, irrespective of the choice of σ^2 , it is that $TF_{f_{2,l}} < TF_{f_1} = \sqrt{2/\pi}$, and the $TF_{f_{2,l}}$ sequence is decreasing, namely, it can be verified that $\{TF_{f_{2,l}} : 1 \leq l \leq 4\} = \{0.58, 0.53, 0.49, 0.46\}$.

The motivation for a Bayesian *nonparametric* framework for noise reduction comes from the fact that the application of stochastic methods, under the false assumption of a normal noise process ($f = f_1$), will artificially enlarge the estimated variance of the presumed normal errors, thus, causing poor inference for the system parameters of interest, as demonstrated in Ref. [23].

3 The dynamic noise reduction replicator model

In this work, given a noisy corrupted time series x^n , we will use a Bayesian nonparametric approach to estimate the posterior joint density of a noise reduced vector of random variables $Y^n = (Y_1, \dots, Y_n)$. A noise reduced time series $y^n = (y_1, \dots, y_n)$, will be formed by some central tendency statistic applied to predictive samples of the marginal posterior densities (MPDs) for all $i = 1, \dots, n$. We define, the estimated vectors $\hat{\theta}_{x^n}$ and $\hat{\theta}_{y^n}$, of the control parameters of g , and the associated estimated noise components \hat{f}_{x^n} and \hat{f}_{y^n} , based on the time series x^n and y^n , respectively. Our intention is to create the y^n time series, in such a way, that it possesses an underlying estimated deterministic law, $\hat{g}_{y^n}(\cdot) := g(\hat{\theta}_{y^n}, \cdot)$, that is in some sense (to be made precise in the sequel) close to the estimated deterministic law, $\hat{g}_{x^n}(\cdot) := g(\hat{\theta}_{x^n}, \cdot)$, responsible for x^n , such that, the estimated noise component \hat{f}_{y^n} influencing interactively the y^n time series, will be a weaker version of the estimated dynamic noise component \hat{f}_{x^n} influencing the original x^n time series. We remark that the \hat{g}_{y^n} and \hat{f}_{y^n} estimations under the noise reduced trajectory y^n have been produced via the GSBR-sampler in Ref. [23].

3.1 A generic probability model

To permit a stochastic approach to the estimation of the unobserved sequence y^n , under the generic assumption of a symmetric zero mean dynamical error process, we adopt the following

stochastic model:

$$\begin{aligned}
x_i &= g(\theta, x_{i:d}) + e_i, \quad e_i \stackrel{\text{i.i.d.}}{\sim} f(\cdot) \\
f(\cdot) &= \sum_{k=1}^{\infty} w_k \mathcal{N}(\cdot | 0, \lambda_j^{-1}), \quad 1 \leq i \leq n \\
y_i &= g(\theta, y_{i:d}) + \zeta_i, \quad \zeta_i \stackrel{\text{i.i.d.}}{\sim} \mathcal{N}(\cdot | 0, \delta) \\
y_{1:d} &= x_{1:d}, \quad \text{P - a.s.} \quad \text{and} \quad |x_i - y_i| < \gamma_i, \quad \gamma_i \stackrel{\text{i.i.d.}}{\sim} h(\cdot),
\end{aligned} \tag{5}$$

where we define $w^\infty = (w_k)_{k \geq 1}$ to be an infinite sequence of random probability weights, $\lambda^\infty = (\lambda_k)_{k \geq 1}$ an infinite sequence of independent and identically distributed (i.i.d) positive random variables (the precisions), with the two sequences w^∞ and λ^∞ independent of each other. The positive random variables γ_i are i.i.d. from some distribution h , possibly depending on parameters.

We will show numerically, that under a reasonable choice for the prior distribution of the variable $\tau = \delta^{-1}$, the posterior distribution of δ (the variance), will concentrate its mass near zero. This, will enable us, to minimize the overall deviation of the y^n trajectory from the estimated determinism. To control the similarity of the y^n trajectory, with respect to the observed x^n trajectory, we assume that both trajectories originate from the same initial point, that is, $y_{1:d} = x_{1:d}$. At the same time, a-priori, we restrict each y_i to be γ_i -close to x_i . The latter statement, conveys prior information, on the *proximity* of the variable y_i to the data point x_i . Finally, we remark that the random mixture $\omega \mapsto f(\cdot, \omega) = \sum_{k=1}^{\infty} w_k(\omega) \mathcal{N}(\cdot | 0, \lambda_j^{-1}(\omega))$ undertakes the rôle of a nonparametric prior over the noise density assumed responsible for the time series x^n , supported over the space of densities with mean zero, which are in turn supported over \mathbb{R} .

We note the following lemma, which will prove useful in the sequel:

Lemma 2. *Letting $\mathcal{P} := \cap_{i=1}^n \{|x_i - y_i| < \gamma_i\}$, we have the following cases:*

1. *When $\gamma_i = \bar{\gamma}_i = \text{const. a.s.}$ for $1 \leq i \leq n$, it is that*

$$\text{P}(\mathcal{P} | x^n, y^n) = \prod_{i=1}^n \mathcal{I}(x_i - \bar{\gamma}_i < y_i < x_i + \bar{\gamma}_i).$$

2. *If $\gamma_i \stackrel{\text{i.i.d.}}{\sim} \mathcal{W}(2, \sqrt{2/\rho})$ for $1 \leq i \leq n$, where ρ is a fixed hyperparameter, and $\mathcal{W}(a, b)$ denotes the Weibull distribution of shape a and scale b , we have that*

$$\text{P}(\mathcal{P} | x^n, y^n) = \exp \left\{ -\frac{\rho}{2} \sum_{i=1}^n (x_i - y_i)^2 \right\}.$$

Proof: (1.) When $\gamma_i = \bar{\gamma}_i$ for all $1 \leq i \leq n$, it is that

$$\text{P}(\mathcal{P} | x^n, y^n) = \begin{cases} 1 & y_i \in (x_i - \bar{\gamma}_i, x_i + \bar{\gamma}_i), \quad 1 \leq i \leq n \\ 0 & \text{otherwise.} \end{cases}$$

(2.) Because $\gamma_i \stackrel{\text{i.i.d.}}{\sim} \mathcal{W}(2, \sqrt{2/\rho})$ if and only if $\gamma_i^2 \stackrel{\text{i.i.d.}}{\sim} \mathcal{E}(\rho/2)$, where $\mathcal{E}(a)$ denotes the exponential distribution with mean $1/a$, it is that

$$\mathbb{P}(\mathcal{P} | x^n, y^n) = \prod_{i=1}^n \mathbb{P}\{\gamma_i^2 > (x_i - y_i)^2\} = \prod_{i=1}^n \exp\{-\rho(x_i - y_i)^2/2\},$$

which gives the desired result. \square

3.2 The posterior model

We consider the posterior of the stochastic quantities f , θ , $x_{1:d}$, $y_{1:d}$, τ and y^n given the data set x^n , the restriction $\mathcal{R} := \{y_{1:d} = x_{1:d}\}$, the proximity information \mathcal{P} , and the model space \mathcal{M} for the functional representation of the deterministic part $g(\theta, x_{i:d})$; for example, the model space could be the ring $\mathbb{R}[x_{i:d}]$ of polynomial functions in the variable $x_{i:d}$, with coefficients over \mathbb{R} . Then, using Bayes' theorem, we have

$$\begin{aligned} \pi(f, \theta, x_{1:d}, y_{1:d}, \tau, y^n | x^n, \mathcal{R}, \mathcal{P}, \mathcal{M}) &\propto \\ \pi(f, \theta, x_{1:d}, y_{1:d}, \tau) &\pi(y^n, x^n, \mathcal{R}, \mathcal{P} | f, \theta, x_{1:d}, y_{1:d}, \tau, \mathcal{M}), \end{aligned} \quad (6)$$

where $\pi(f, \theta, x_{1:d}, y_{1:d}, \tau)$ is the prior density. Having in mind, that the estimation of the noise density f is equivalent to the estimation of the variables w^∞ and λ^∞ , the likelihood factor on the second line of equation (6), becomes

$$\begin{aligned} \pi(y^n, x^n, \mathcal{R}, \mathcal{P} | w^\infty, \lambda^\infty, \theta, x_{1:d}, y_{1:d}, \tau, \mathcal{M}) &= \\ \mathbb{P}(\mathcal{R} | y_{1:d}, x_{1:d}) \mathbb{P}(\mathcal{P} | x^n, y^n) &\pi(x^n | w^\infty, \lambda^\infty, \theta, x_{1:d}, \mathcal{M}) \pi(y^n | \theta, \tau, y_{1:d}). \end{aligned} \quad (7)$$

We believe, that it will be more efficient to control the average corrections between the two trajectories, under the assumption that $\gamma_i^2 \stackrel{\text{i.i.d.}}{\sim} \mathcal{E}(\rho/2)$. For this reason, we augment the conditional part of our posterior by the hyperparameter ρ . Then, taking into account the model representation for the noise components in (5), lemma 2, the fact that $\mathbb{P}(\mathcal{R} | y_{1:d}, x_{1:d}) = \mathcal{I}(y_{1:d} = x_{1:d})$ and the likelihood representation in (7), the posterior becomes

$$\begin{aligned} \pi(w^\infty, \lambda^\infty, \theta, x_{1:d}, \tau, y^n | x^n, \mathcal{R}, \mathcal{P}, \mathcal{M}, \rho) &\propto \pi(w^\infty, \lambda^\infty, \theta, x_{1:d}, \tau) \\ &\times \mathcal{I}(y_{1:d} = x_{1:d}) \prod_{i=1}^n \mathcal{N}(y_i | x_i, \rho^{-1}) \prod_{i=1}^n \sum_{j=1}^{\infty} w_j \mathcal{N}(x_i | g(\theta, x_{i:d}), \lambda_j^{-1}) \prod_{i=1}^n \mathcal{N}(y_i | g(\theta, y_{i:d}), \tau^{-1}). \end{aligned}$$

Such a likelihood will lead to a Gibbs sampler with an infinite number of full conditional distributions. To avoid that, we introduce the jointly discrete random vectors $d^n = (d_1, \dots, d_n)$ and $N^n = (N_1, \dots, N_n)$ (see Ref. [23], and references therein). The d_i random variable, denotes the component of the random mixture f in (5), that the observation x_i came from. In fact, the state space of the d_i variable can be made a.s. finite, if we define the random variable $N_i \sim f_N(\cdot | p)$, where p is a parameter, such that, the conditional random variable

$(d_i|N_i)$ attains a discrete uniform distribution over the a.s. finite set $\mathcal{S}_i = \{1, \dots, N_i\}$. Then, it can be shown, that by letting N_i to follow the particular negative binomial distribution $f_N(N_i|p) = N_i p(1-p)^{N_i-1} \mathcal{I}(N_i \geq 1)$, the random weights w_j in (5), will form the strictly decreasing geometric sequence $w_j = p(1-p)^{j-1} \mathcal{I}(j \geq 1)$. So that, in the (d^n, N^n) -augmented posterior (6), we can switch from the variable w^∞ to the variable p . Finally, the posterior attains the representation

$$\begin{aligned} \pi(p, \lambda^\infty, d^n, N^n, \theta, x_{1:d}, \tau, y^{(n)} | x^{(n)}, \rho, \mathcal{R}, \mathcal{P}, \mathcal{M}) &\propto \pi(p, \lambda^\infty, \tau, \theta, x_{1:d}) \\ &\times \prod_{\substack{i=1 \\ d_i: d_i \leq N_i}}^n p^2(1-p)^{N_i-1} \lambda_{d_i}^{1/2} \exp \left\{ -\frac{\lambda_{d_i}}{2} (x_i - g(\theta, x_{i:d}))^2 \right\} \\ &\times \mathcal{I}(y_{1:d} = x_{1:d}) \tau^{n/2} \exp \left\{ -\frac{1}{2} \sum_{i=1}^n [\tau(y_i - g(\theta, y_{i:d}))^2 + \rho(y_i - x_i)^2] \right\}. \end{aligned} \quad (8)$$

We note that, the likelihood factor in the second line of the previous equation, is very similar to the GSBR-likelihood that appears in equation (11), of Proposition 1, in Ref. [23].

3.3 Priors and full conditional distributions

To complete the model, we assign independent priors to the variables p , λ^∞ , θ , $x_{1:d}$, and τ , namely:

1. We set $\pi(p) = \mathcal{B}(p|a_1, a_2)$, a beta conjugate prior, with fixed shape hyperparameters a_1 and a_2 .
2. The variable λ^∞ is an infinite sequence of independent precisions (inverse variances). Nevertheless, the nonparametric MCMC will require, at each sweep, the computation of only an almost surely *finite* number, $N^* = \max_{1 \leq k \leq n} N_k$, of posterior λ_j s. Standard Bayesian modeling suggests to use gamma conjugate prior distributions over the λ_j precision parameters, so we set $\Pi(d\lambda^\infty) = \prod_{j=1}^\infty \mathcal{G}(\lambda_j|b_1, b_2) d\lambda_j$, where b_1 and b_2 are the fixed shape and rate hyperparameters, respectively. Similarly, because τ is a precision, we set a-priori $\pi(\tau) = \mathcal{G}(\tau|\gamma_1, \gamma_2)$.
3. For the vector of parameters $\theta = (\theta_1, \dots, \theta_s)$ and for the the vector of initial conditions $x_{1:d} = (x_0, \dots, x_{1-d})$, we assume the independent priors $\pi(\theta) \propto 1$ and $\pi(x_{1:d}) \propto 1$, respectively. For example, suppose that a-priori we have

$$\pi(\theta_1, \dots, \theta_s) \propto \prod_{i=1}^s \exp\{-(\theta_i - \theta_{0,i})^2 / 2\sigma_{0,i}^2\},$$

then letting $\sigma_{0,i}^2$ tend to infinity, one obtains $\pi(\theta) \propto 1$. Such a prior is noninformative, and although improper (not a density over \mathbb{R}^s), leads to a proper full conditional for θ .

Note that, to reduce dynamical error, the prior expectation $\mathbb{E}(\delta)$ will have to be set close to zero. And if at the same time, we want to control the proximity between the original and the noise reduced orbit, we will have to predetermine values for the prior means of γ_i s, in the interval $[2 \times 10^{-6}, 2 \times 10^{-4}]$. This is due to the fact, that the individual distances $|x_i - y_i|$ are by construction small.

We have the following proposition:

Proposition 1. *The full conditional distributions for the noise reduced orbit y^n , are given by $\pi(y_j | \dots) \propto e^{-C(y_j | \dots)/2}$, where $\pi(y_j | \dots)$ denotes the dependence of the variable y_j to the rest of the variables. Letting $h_\theta(y_j, y_{j:d}) := (y_j - g(\theta, y_{j:d}))^2$, the function $C(y_j | \dots)$, for $j = 1, \dots, d$ is given by*

$$C(y_j | \dots) = \tau \sum_{k=0}^d h_\theta(y_{j+k}, y_{j+k:d}) \\ \times \mathcal{I}(y_0 = x_0, \dots, y_{-d+j} = x_{-d+j}) + \rho(y_j - x_j)^2,$$

for $j = d+1, \dots, n-d$ is given by

$$C(y_j | \dots) = \tau \sum_{k=0}^d h_\theta(y_{j+k}, y_{j+k:d}) + \rho(y_j - x_j)^2,$$

and, for $j = n-d+1, \dots, n$, by

$$C(y_j | \dots) = \tau \sum_{k=0}^{j-n} h_\theta(y_{j+k}, y_{j+k:d}) + \rho(y_j - x_j)^2.$$

Proof: The desired result, comes from the representation of the posterior in equation (8). \square

3.4 The DNRR sampler

To accelerate the convergence of the Gibbs sampler based on the posterior distribution in (8), we collect our variables in to the two groups:

$$G_1 = \{v, \theta, x_{1:d}\} \quad \text{and} \quad G_2 = \{\tau, y^n\}$$

with $v = \{p, \lambda^\infty, d^n, N^n\}$. We first sample, from the full conditionals of G_1 given x^n , and then, from the full conditionals of G_2 given G_1 and x^n . Then, it is not difficult to see that such a *blocked* Gibbs sampler scheme, admits the same stationary distribution as the plain Gibbs sampler scheme, coming from sampling the full conditionals of $G_1 \cup G_2$ given x^n , each one individually.

Proposition 2. *Given the model \mathcal{M} and fixed $\rho > 0$, marginally, $(G_2 | x^n)$ is distributed as*

$$(G_2 | x^n) \sim \int_{\mathbb{R}^{s+d} \times \mathbb{V}} \Pi(\cdot, \cdot | \theta, x_{1:n}, x^n) \Pi(d\theta, dx_{1:n} | v, x^n) \Pi(dv | x^n), \quad (9)$$

where \mathbb{V} denotes the support of the random vector v .

Proof: Given the model \mathcal{M} , and fixed $\rho > 0$, we want to sample from the variable $(\tau, y^n | x^n)$. To do so, we should first sample from the joint of θ and $x_{1:n}$ given x^n , and then from the joint of τ and y^n given θ and $x_{1:n}$, that is

$$(\theta, x_{1:n} | x^n) \sim \Pi(\cdot, \cdot | x^n)$$

and then from

$$(\tau, y^n | x^n) \sim \Pi(\cdot, \cdot | \theta, x_{1:n}, x^n)$$

whence

$$(\tau, y^n | x^n) \sim \int_{\mathbb{R}^{s+d}} \Pi(\cdot, \cdot | \theta, x_{1:n}, x^n) \Pi(d\theta, dx_{1:n} | x^n).$$

For a generic noise source, we have to sample first from $(p, \lambda^\infty | x^n)$, and then from $(\theta, x_{1:n} | p, \lambda^\infty, x^n)$. However, for the creation of an a.s. finite Gibbs sampler, the random vector (d^n, N^n) has to be introduced. Then, letting $v = (p, \lambda^\infty, d^n, N^n)$, one has

$$(\theta, x_{1:n} | x^n) \sim \int_{\mathbb{V}} \Pi(\cdot, \cdot | v, x^n) \Pi(dv | x^n),$$

which gives the desired result. \square

Now, it is clear, that our model is based on the iteration of two consecutive steps, the $(\hat{g}_{x^n}, \hat{f}_{x^n})$ -reconstruction step and the y^n -sampling step:

1. We have seen that the reconstruction step, stems from the GSBR-sampler introduced in Ref. [23]. The differences are: the absence of the out-of-sample variables, the more general d -dimensional lag dependence, the application of a conjugate beta prior and the application of an improper prior, on the variables p and $(\theta, x_{1:d})$, respectively.
2. In the noise-reduction step, the noise reduced trajectory y^n , is sampled conditionally on the sampled values of the reconstruction step. We can think of the reconstruction stage, as providing observations from the *distributions* of the initial condition $y_{1:n}$ and the parameter θ of the estimated deterministic part \hat{g}_{x^n} of the new trajectory. To replicate the \hat{g}_{x^n} -dynamics, under a reduced dynamical error, we use a Metropolis within Gibbs updating procedure, with a small variance random walk proposal distribution, initialized at the observed x^n trajectory.

Then, the new trajectory y^n , has the following properties:

1. We define, the relative dynamical noise reduction R_{dyn} attained by the y^n trajectory with respect to the y^n as

$$R_{\text{dyn}}(y^n, x^n; \hat{g}_{x^n}) := 1 - \frac{E_{\text{dyn}}(y^n; \hat{g}_{x^n})}{E_{\text{dyn}}(x^n; \hat{g}_{x^n})},$$

so that $R_{\text{dyn}} > r$ implies $E_{\text{dyn}}(y^n; \hat{g}_{x^n}) < (1 - r)E_{\text{dyn}}(x^n; \hat{g}_{x^n})$. We will see, that in all our numerical examples, it is that with $r > 0.8$.

2. When ρ tends to infinity, the distribution of distances between the individual points of the y^n and x^n trajectories, concentrates its mass to zero.
3. The estimated underlying deterministic parts of y^n and x^n are close to each other. For suppose, that we estimate in terms of the GSBR-sampler, the g -dynamics given the x^n and the y^n trajectories. Then the distance $d(\hat{g}_{x^n}, \hat{g}_{y^n})$ between the two deterministic parts will be small; for example, when \hat{g}_{x^n} and \hat{g}_{y^n} are polynomials, this distance could be the l_2 -norm of the polynomial $\hat{g}_{x^n} - \hat{g}_{y^n}$.

The sampling scheme: We first specify initial values for the variables $x_{1:n}$, θ , τ , and we iterate for $t = 1, \dots, K$ the following sampling scheme:

- S1: For $i = 1, \dots, n$, generate the state space range variable $N_i^{(t)} \sim \pi(N_i | \dots)$, of the allocation variable $d_i^{(t)}$.
- S2: For $i = 1, \dots, n$, generate the infinite mixture allocation variable $d_i^{(t)} \sim \pi(d_i | \dots)$.
- S3: For $i = 1, \dots, N^*$, with $N^* = \max_{1 \leq k \leq n} N_k$, sample $\lambda_i^{(t)} \sim \pi(\lambda_i | \dots)$.
- S4: Generate the initial condition vector $(x_{1:n})^{(t)} \sim \pi(x_{1:n} | \dots)$
- S5: Generate $\theta^{(t)} \sim \pi(\theta | \dots)$.
- S6: Sample the geometric probability $p^{(t)} \sim \pi(p | \dots)$.
- S7: Having updated $p^{(t)}$ and $\lambda^{(t)}$ up to N^* , sample from the noise process \hat{f}_{x^n}

$$z_{n+1}^{(t)} \sim \sum_{j=1}^{N^*} p^{(t)} (1 - p^{(t)})^{j-1} \mathcal{N}(z_{n+1} | 0, 1/\lambda_j^{(t)}).$$

- S8: Initialize the vector of initial conditions $(y_{1:n})^{(t)}$ of the noise reduced trajectory to the previously sampled initial condition $(x_{1:n})^{(t)}$ of the x^n , and iterate for $j = 1, \dots, n$ the following Metropolis-within-Gibbs sampling scheme:

- (a) Generate proposal

$$y_j^* \sim y_j^{(t-1)} + \nu \mathcal{N}(0, 1). \quad (10)$$

- (b) Calculate the acceptance probability $\alpha(y_j^{(t-1)}, y_j^*)$ given by

$$\min \left\{ 1, \exp \left\{ -\frac{1}{2} \left[C(y_j^* | \dots) - C(y_j^{(t-1)} | \dots) \right] \right\} \right\}.$$

- (c) Accept $y_j^{(t)} = y_j^*$ with probability $\alpha(y_j^{(t-1)}, y_j^*)$.

- S9: Generate $\tau^{(t)} \sim \pi(\tau | \dots)$.

4 Simulation Results

In this section, we will provide numerical illustrations of the DNRR algorithm for the random Hénon map, and the random bistable cubic map introduced in Ref. [23]. In all cases, except in the case for the variable τ , the prior specifications are completely noninformative.

As a prior for the geometric probability variable, we take the arcsine density $p \sim \mathcal{B}(0.5, 0.5)$, which coincides with the Jeffrey's prior for p . On the precisions $(\lambda_j)_{j \geq 1}$ of the random density f , we place the vague gamma prior $\lambda_j \sim \mathcal{G}(10^{-3}, 10^{-3})$, which is very close to a scale invariant prior. On the control variable θ , and the initial condition variable $x_{1:d}$, we assign the translation invariant priors $\pi(\theta) \propto 1$ and $\pi(x_{1:d}) \propto 1$, respectively. Because we want a-posteriori to force the variance $\delta = \tau^{-1}$ to concentrate its mass near zero, we have to set its prior mean and variance close to zero. We can achieve this by setting $\tau \sim \mathcal{G}(10^4, 10^{-2})$. Finally, to avoid mixing issues, following standard methodology, each time, we calibrate [27] the proposal variance ν^2 of the embedded Metropolis-within-Gibbs sampler in equation (10), such that, the mean acceptance probability of the sampling scheme is between 25 and 35%.

In all our numerical experiments, the DNRR Gibbs samplers have ran for 25×10^4 iterations leaving the first 5×10^4 samples as a burn-in period.

4.1 The Hénon map

We consider a time series realization x^n of size $n = 1000$, coming from the random recurrence relation given in (2) with $e_i \stackrel{\text{i.i.d.}}{\sim} f_{2,1}$, variance $\sigma^2 = 0.21 \times 10^{-4}$ and initial condition $x_0 = x_{-1} = 0.5$ for noise level at approximately 3%. We model the deterministic part g , with the complete quadratic polynomial in the two variables, namely

$$g(\theta, x_{i-1}, x_{i-2}) = \theta_0 + \theta_1 x_{i-1} + \theta_2 x_{i-2} + \theta_3 x_{i-1} x_{i-2} + \theta_4 x_{i-1}^2 + \theta_5 x_{i-2}^2. \quad (11)$$

1. A neutral proximity restriction: We first ran the DNRR sampler with the proximity parameter set to $\rho = 10^2$. In fact, values of ρ smaller than 10^4 , due to the informative nature of τ , have a diminishing effect on the full conditional distributions of the Y_j variables of proposition 1. As a result, for such ‘small’ ρ values, the proximity restriction \mathcal{P} becomes neutral, and the DNRR sampler estimates the noise reduced orbit y^n attaining minimum average deviation E_{dyn} with respect to the estimated \hat{g}_{x^n} , and maximum average distance with respect to x^n .

In the first two rows of Table 2, we present *percentage absolute relative errors* (PAREs) of the estimated θ -coefficients, with respect to the true values, based on the noisy and the noise reduced trajectories, of the maps \hat{g}_{x^n} and \hat{g}_{y^n} , respectively. The last two columns of the table, display average PAREs, $\bar{\theta}$, and l^2 -distances. Because the y^n based quantities, $\bar{\theta}$ and l^2 , are small, we consider both x^n and y^n based θ -estimations as identifying the specific Hénon map given in (2).

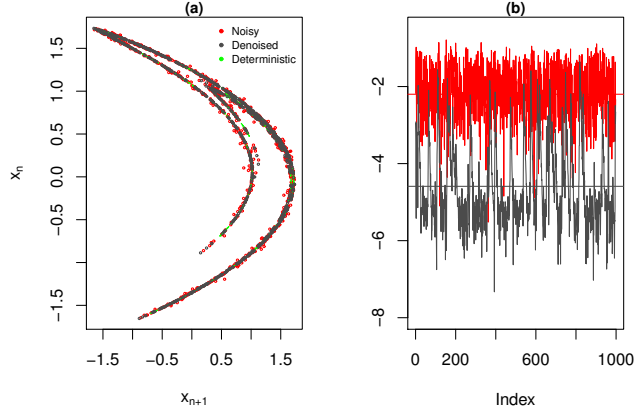


Figure 2: In figure (a), we present superimposed delay plots of the noisy, the noise reduced and the deterministic trajectories of the Hénon map, of length $n = 1000$. The associated \log_{10} -determinism plot is given in figure (b).

Table 1: Relative dynamical noise reductions, average indeterminisms and average distances, for two different values of ρ .

ρ	$E_{\text{dyn}}(x^n, \hat{g}_{x^n})$	$E_{\text{dyn}}(y^n, \hat{g}_{x^n})$	R_{dyn}	E_0
10^2	0.02932	0.00286	0.9023	0.0428
5×10^5	0.02932	0.00710	0.7577	0.0223

The posterior variance $\delta = \tau^{-1}$ has the interval $[1.39 \times 10^{-6}, 1.81 \times 10^{-6}]$ as a 95% highest posterior density interval. The distribution of the individual variances of the y^n trajectory, concentrates most of its mass in the interval $[0, 10^{-5}]$.

We have the following results presented from Figure 2 to Figure 6:

1.1. Noise reduction measures: In Figure 2(a), we present superimposed the original time series x^n (points in red), and the estimated noise reduced trajectory y^n (points in dark gray) in delay coordinates. We can see the noise reduced trajectory, shadowing the original trajectory, in the regions of noise-induced prolongations. In Figure 2(b), we display superimposed the individual \log_{10} -determinism plots of the original and the estimated time series, in red and dark gray color, respectively; for example, the individual \log_{10} -determinism plot of the time series (x_i) is the trace of time series $(\log_{10} |E_{\text{dyn}}(x_i, \hat{g})|)$. The red and black horizontal lines correspond to the average \log_{10} -determinisms of the noisy and the noise reduced times series, respectively. In the first line of Table 1, we exhibit the denoising measures E_{dyn} , R_{dyn} and E_0 . The average noise reduction achieved by the DNRR sampler is larger than two orders of magnitude, with $R_{\text{dyn}}(y^n, x^n; \hat{g}_{x^n}) = 0.902$, $E_{\text{dyn}}(y^n; \hat{g}_{x^n}) = 0.00286$ and $E_0(x^n, y^n) = 0.0428$.

1.2. Dynamic noise estimation: In Figure 3, we display superimposed the true noise density $f = f_{2,1}$ (red continuous curve), the x^n based estimated noise density \hat{f}_{x^n} (black continuous

Table 2: PAREs, average PAREs and l^2 -distances, for the estimated coefficients of the deterministic part of the perturbed Hénon map in (2), based on the noisy and the corresponding noise reduced trajectories, for two different values of ρ .

Time series	ρ	θ_0	θ_1	θ_2	θ_3	θ_4	θ_5	$\bar{\theta}$	l^2
x^n	10^2	0.089	0.096	0.046	0.044	0.011	0.070	0.059	0.00177
y^n		0.063	0.043	0.022	0.028	0.020	0.038	0.036	0.00110
x^n	5×10^5	0.079	0.071	0.041	0.031	0.002	0.059	0.047	0.00146
y^n		0.177	0.155	0.015	0.023	0.005	0.157	0.089	0.00330

curve) and the y^n based estimated noise density \hat{f}_{y^n} (black dashed curve). We remark the closeness of the noise densities f and \hat{f}_{x^n} , and the fact that the \hat{f}_{y^n} density, represents a much ‘weaker’ error process. The latter, along with the fact that the θ -estimation based on the noise reduced trajectory identifies the specific Hénon map, validates our contention, that the noise reduced trajectory comes from a dynamical system very close to the original one, perturbed interactively by a ‘weaker’ error process.

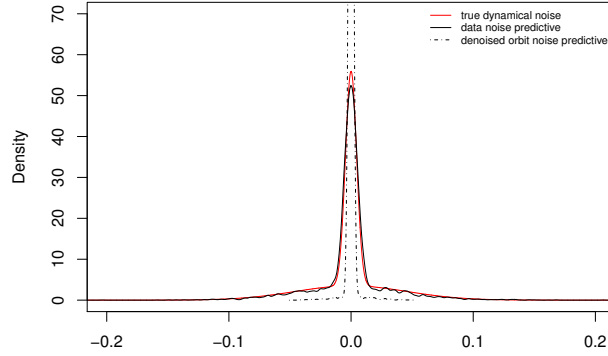


Figure 3: The true noise density $f = f_{2,1}$, for $\sigma^2 = 0.21 \times 10^{-4}$, is the red continuous curve. Along, we superimpose the x^n -estimated noise density \hat{f}_{x^n} as a black continuous curve, and the y^n -estimated ‘weaker’ interactive noise density \hat{f}_{y^n} as a black dashed curve.

1.3. The existence of HTs as a cause for a-posteriori multimodality: While most of the Y_i -MPDs are unimodal, a small number of them is multimodal, namely, those that their support contains the projection of a point of HT. We have used the Hartigan’s statistical test [12] for multimodality, to choose the appropriate Y_i -point estimator; we utilize the maximum a-posteriori (MAP) estimator for the case of a Y_i -multimodal MPD, and the sample mean estimator for the unimodal case. In Figure 4(a) we present a delay plot of the set M_{HT} of MAP estimations (solid red circles) coming from the Y_i -posterior marginals, passing the Hartigan’s test for multimodality. Alternatively, we could consider the Y_i -predictive-samples, coming from the embedded Metropolis-within-Gibbs sampler, after burn-in. For each Y_i -sample, we compute

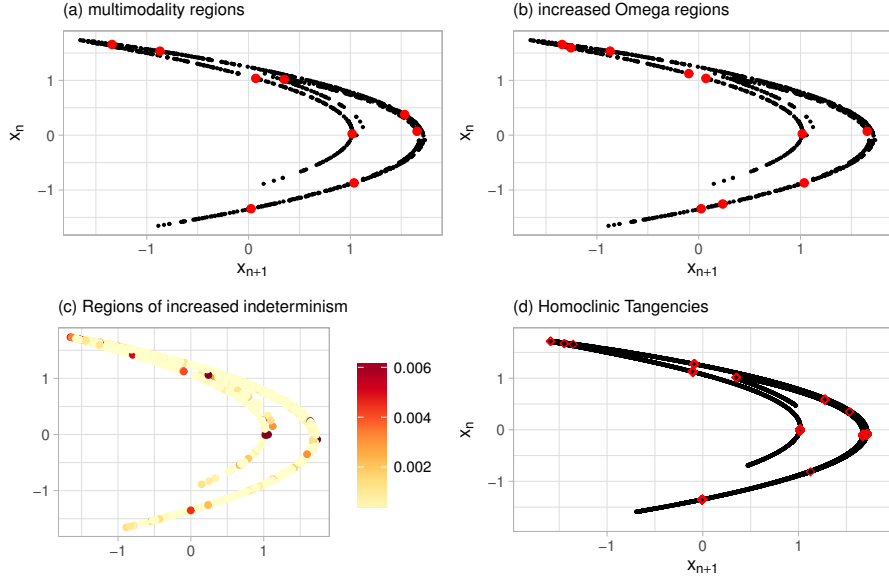


Figure 4: In Figure (a) we present a delay plot of the points in the set M_{HT} of the point estimators of the Y_i -posterior marginals, passing Hartigan’s test for unimodality. In Figure (b) we depict the delay plot of the points in the set Ω_{HT} that are above the 99th percentile of the histogram of Ω . Regions of high E_{dyn} are depicted in Figure (c), and in Figure (d) we present the primary homoclinic tangencies of the corresponding deterministic attractor.

the forecastable component analysis index Ω_i [9, 10], which is normalized in the interval $[0, 1]$. We let $\Omega = \{\Omega_i : 1 \leq i \leq n\}$, and we consider the subset of points Ω_{HT} of Ω , that are above the 99th percentile of its histogram, and thus, their predictive distribution exhibits *more structure*. In Figure 4(b) we depict a delay plot of Ω_{HT} (solid red circles). We can see that the points in the sets M_{HT} and Ω_{HT} are related to the areas of increased indeterminism depicted in Figure 4(c). The location of the deterministic primary HTs are given in Figure 4(d). We remark that the sets M_{HT} and Ω_{HT} , for fixed n , are random (point process realizations) because they depend on the particular realization of the time series x^n , for example $\omega \mapsto \Omega_{HT} = \Omega_{HT}(y^n|x^n(\omega))$.

2. The average distance E_0 as a function of ρ : Here we perform a series of executions of the DNRR sampler with the same prior set up, and the same observed time series x^n , as in the previous subsection, for different values of the ρ parameter. We have taken $\rho \in \{\rho_j = j \times 10^4 : j = 1, \dots, 200\}$. For example, for $\rho = 5 \times 10^5$, the effect of the proximity restriction becomes very strong. In the second line of Table 1, we present the noise reduction measures E_{dyn} , R_{dyn} and E_0 . The average noise reduction achieved in this case decreases to $R_{dyn}(y^n, x^n; \hat{g}_{x^n}) = 0.7577$. The average indeterminism of y^n with respect to \hat{g}_{x^n} escalates to $E_{dyn}(y^n; \hat{g}_{x^n}) = 0.00710$, with the average distance decreased considerably to $E_0(x^n, y^n) = 0.0223$. In Figure 5(a), we present superimposed, the distributions of the individual \log_{10} -indeterminisms of the noise reduced trajectory with respect to \hat{g}_{x^n} , for $\rho = 10^2$ (curve in black) and $\rho = 5 \times 10^5$ (curve in grey). We can see that for large values of ρ the density of \log_{10} -indeterminisms becomes more peaked and

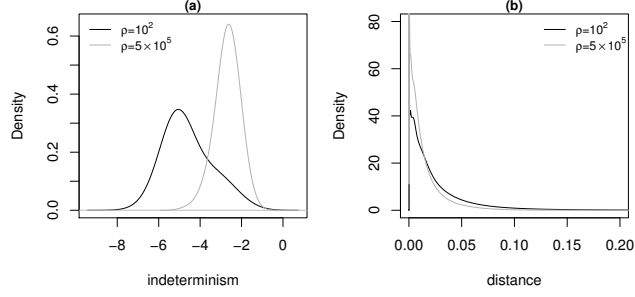


Figure 5: KDEs of (a) individual \log_{10} -indeterminism points and (b) distance between original and noise reduced orbit points, for different values of parameter ρ .

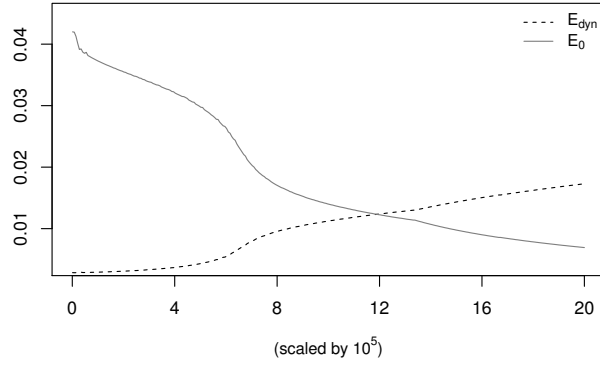


Figure 6: The average distance $E_0(y^n, x^n)$ and the average dynamic error $E_{\text{dyn}}(y^n, \hat{g}_{x^n})$ as functions of the parameter ρ .

shifts to the right. In Figure 5(b), the density of the individual distances for the large value of ρ concentrates its mass near zero.

In Figure 6, we present the noise reduction measures $E_{\text{dyn}}(y^n, \hat{g}_{x^n})$ and $E_0(y^n, x^n)$ as functions of ρ . It is that as ρ increases, the average indeterminism and the average distance are increasing and decreasing, respectively.

3. Fixed noise levels imply fixed relative noise reduction: In this experiment we choose the variances and the time series realizations x^n , for each $f_{2,l}$ noise process for $1 \leq l \leq 4$, such that, they give an associated noise level η of about 3%. In the fourth column of Table 3, we can see that the relative noise reduction measure R_{dyn} , does not undergo major changes, and it attains values between 0.871 and 0.902.

4.2 A bistable cubic map

Here, we consider the cubic map

$$x_i = g(\vartheta, x_{i-1}) = 0.05 + \vartheta x_{i-1} - 0.99x_{i-1}^3. \quad (12)$$

For $\vartheta \in \Theta_{\text{bi}} = [1.27, 2.54]$ the map is bistable in the sense that two mutually exclusive period-doubling cascades coexist. For values of ϑ close to 2.54, we denote the two coexisting attractors

Table 3: Measures of reconstruction and noise reduction efficiency for the $f_{2,l}$ noise processes. The variances of the noise processes, and each realization has been chosen, such that, η is fixed at about 3%, where $E_{\text{dyn}} = E_{\text{dyn}}(y^n, \hat{g}_{x^n})$.

Noise	$\sigma^2 \times 10^4$	E_0	E_{dyn}	R_{dyn}	$\bar{\theta}_{x^n}$	$\bar{\theta}_{y^n}$
$f_{2,1}$	0.21	0.0428	0.00286	0.902	0.059	0.036
$f_{2,2}$	0.29	0.0514	0.00371	0.871	0.115	0.062
$f_{2,3}$	0.40	0.0490	0.00392	0.871	0.072	0.098
$f_{2,4}$	0.77	0.0627	0.00323	0.892	0.054	0.059

by $\mathcal{O}_1 \subset I_1$ and $\mathcal{O}_2 \subset I_2$, with approximately $I_1 = [-1.60, -0.10]$ and $I_2 = [-0.10, 1.67]$. For values of ϑ slightly larger than 2.54, the set \mathcal{O}_2 undergoes a sudden change. It becomes repelling, and all trajectories over $I_1 \cup I_2$ are attracted by \mathcal{O}_1 . In fact, similar behavior can be observed for all $\vartheta \in (2.54, 2.65)$.

We let $\vartheta = \vartheta^* = 2.55$ and we consider the dynamically perturbed map $x_i = g(\vartheta^*, x_{i-1}) + e_i$ with $e_i \stackrel{\text{i.i.d.}}{\sim} f_{2,1}$, $\sigma^2 = 0.55 \times 10^{-4}$, and $\rho = 10^2$. Then, *noise-induced jumps* are taking place between the intervals I_1 and I_2 . Here we consider dynamically perturbed time series observations x^n , of small sample size $n = 200$. As a modeling polynomial, we utilize the general quintic polynomial $g(\theta, x_{i-1}) = \sum_{k=0}^5 \theta_j x_{i-1}^k$.

Noise reduction in the neighborhood of noise induced jumps: In Figure 7(a), we can see the estimated y^n trajectory (in black) evolving in the neighborhood of the original trajectory x^n (in red), incorporating the weaker dynamical noise \hat{f}_{y^n} , given in Figure 8, as a black dashed density. We remark, that our method, is based on the fact that it allows only small stochastic steps around the original orbit, and thus, the noise reduced orbit follows closely the original orbit even to its noise-induced prolongations in the interval I_2 . The corresponding \log_{10} indeterminism plot is given in Figure 7(b). The plot of the individual distances between the original and the noise reduced trajectory is given in Figure 7(c). In Table 4 we display the noise reduction efficiency for the cubic map, for noise levels between 3.5% and 7.5%. In the last column of the table are displayed the average PAREs $\bar{\theta}_{y^n}$ of the y^n based estimation of the deterministic part of the noise reduced dynamics. We have observed, that the average PARE becomes larger than 1%, when the noise level exceeds 8%.

Table 4: Measures of reconstruction and noise reduction efficiency for the cubic map, for various σ^2 's for the $f_{2,1}$ noise processes, where $E_{\text{dyn}} = E_{\text{dyn}}(y^n, \hat{g}_{x^n})$.

$\sigma^2 \times 10^4$	η %	E_0	E_{dyn}	R_{dyn}	$\bar{\theta}_{x^n}$	$\bar{\theta}_{y^n}$
0.33	3.5	0.0395	0.00749	0.812	0.281	0.425
0.55	4.5	0.0413	0.00695	0.842	0.605	0.804
0.59	5.5	0.0631	0.00952	0.826	0.438	0.262
0.67	6.5	0.0453	0.00847	0.848	0.872	0.958
1.00	7.5	0.0630	0.00819	0.867	0.856	0.987

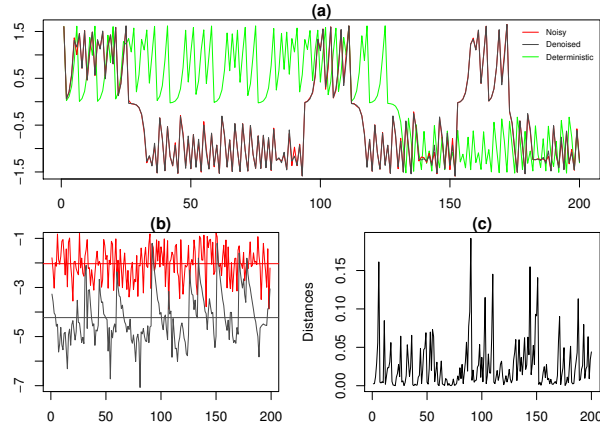


Figure 7: In Figure (a), we give superimposed, the deterministic trajectory, the noisy trajectory x^n and the estimated y^n trajectory. In Figure (b) we present the corresponding \log_{10} indeterminism plot. The trace of the individual distances between the original and the noise reduced trajectory is given in Figure (c).

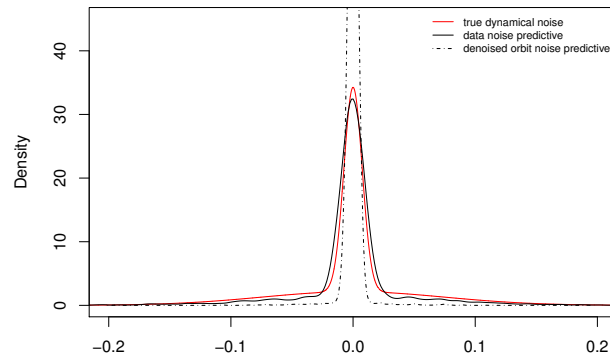


Figure 8: Kernel density estimations based on the predictive samples of \hat{f}_{x^n} (continuous black curve), the predictive samples of \hat{f}_{y^n} (dashed black curve) along with the true dynamical noise density (continuous red curve).

5 Discussion

We have presented, a novel approach to the problem of noise reduction of dynamically perturbed nonlinear maps, the DNRR sampler. Our approach is Bayesian, modeling a noise reduced trajectory y^n , that *evolves in the neighborhood* of a given noisy trajectory x^n . Our proposed DNRR algorithm, is flexible and accurate, because the assumptions for the underlying noise process f perturbing the original trajectory are relaxed. A-priori, we consider the noise as coming from a random countable mixture of zero mean Gaussians. Then, the number of the components, the weights, and the variances of the normal mixture \hat{f}_{x^n} , approximating the actual noise process f , are estimated directly from the observed time series. This in turn, implies a high accuracy estimation of the deterministic part \hat{g}_{x^n} , which is the basic ingredient of the replication part of the DNRR sampler. Also, we have seen, that for moderate noise levels, the noise reduced trajectory y^n , has an estimated deterministic part \hat{g}_{y^n} remaining close to the estimated deterministic part \hat{g}_{x^n} of the original trajectory.

We could modify the proposed DNRR model, by dropping the assumption of a known functional form for the deterministic part, and instead, apply over g , a Gaussian Process prior [25]. We believe, that such an approach, will be appropriate for a wide variety of real world data sets, characterized by strong nonlinearity and (or) complicated contaminating dynamic noise.

References

- [1] L Mark Berliner. Statistics, probability and chaos. *Statistical Science*, pages 69–90, 1992.
- [2] Sangit Chatterjee and Mustafa R Yilmaz. Chaos, fractals and statistics. *Statistical Science*, pages 49–68, 1992.
- [3] ME Davies. Nonlinear noise reduction through monte carlo sampling. *Chaos: An Interdisciplinary Journal of Nonlinear Science*, 8(4):775–781, 1998.
- [4] Mike Davies. Noise reduction by gradient descent. *International Journal of Bifurcation and Chaos*, 3(01):113–118, 1993.
- [5] Mike Davies. Noise reduction schemes for chaotic time series. *Physica D: Nonlinear Phenomena*, 79(2-4):174–192, 1994.
- [6] Arnaud Doucet, Nando De Freitas, and Neil Gordon. An introduction to sequential monte carlo methods. In *Sequential Monte Carlo methods in practice*, pages 3–14. Springer, 2001.
- [7] J Doyne Farmer and John J Sidorowich. Optimal shadowing and noise reduction. *Physica D: Nonlinear Phenomena*, 47(3):373–392, 1991.

- [8] Ruth Fuentes-García, Ramses H Mena, and Stephen G Walker. A new bayesian non-parametric mixture model. *Communications in StatisticsSimulation and Computation*®, 39(4):669–682, 2010.
- [9] Georg M Goerg. Forecastable component analysis. In *ICML (2)*, pages 64–72, 2013.
- [10] Georg M. Goerg. *ForeCA: An R package for Forecastable Component Analysis*, 2016. R package version 0.2.4.
- [11] Stephen M Hammel. A noise reduction method for chaotic systems. *Physics letters A*, 148(8-9):421–428, 1990.
- [12] John A Hartigan and Pamela M Hartigan. The dip test of unimodality. *The annals of Statistics*, pages 70–84, 1985.
- [13] Spyridon J Hatjispyros, Theodoros Nicolieris, and Stephen G Walker. Parameter estimation for random dynamical systems using slice sampling. *Physica A: Statistical Mechanics and its Applications*, 381:71–81, 2007.
- [14] Spyridon J Hatjispyros, Theodoros Nicolieris, and Stephen G Walker. A bayesian nonparametric study of a dynamic nonlinear model. *Computational Statistics & Data Analysis*, 53(12):3948–3956, 2009.
- [15] Lars Jaeger and Holger Kantz. Effective deterministic models for chaotic dynamics perturbed by noise. *Physical Review E*, 55(5):5234, 1997.
- [16] Lars Jaeger and Holger Kantz. Homoclinic tangencies and non-normal jacobians - effects of noise in nonhyperbolic chaotic systems. *Physica D: Nonlinear Phenomena*, 105(1):79–96, 1997.
- [17] Maarten Jansen. *Noise reduction by wavelet thresholding*, volume 161. Springer Science & Business Media, 2012.
- [18] Kevin Judd. Shadowing pseudo-orbits and gradient descent noise reduction. *Journal of Nonlinear Science*, 18(1):57–74, 2008.
- [19] Holger Kantz and Thomas Schreiber. *Nonlinear time series analysis*, volume 7. Cambridge university press, 2004.
- [20] Steven P Lalley et al. Beneath the noise, chaos. *The Annals of Statistics*, 27(2):461–479, 1999.
- [21] Steven P Lalley and Andrew B Nobel. Denoising deterministic time series. *arXiv preprint nlin/0604052*, 2006.

- [22] Alistair I Mees. *Nonlinear dynamics and statistics*. Springer Science & Business Media, 2012.
- [23] Christos Merktas, Konstantinos Kaloudis, and Spyridon J Hatjispyros. A bayesian nonparametric approach to reconstruction and prediction of random dynamical systems. *Chaos: An Interdisciplinary Journal of Nonlinear Science*, 27(6):063116, 2017.
- [24] Edward Ott. *Chaos in dynamical systems*. Cambridge university press, 2002.
- [25] Carl Edward Rasmussen. Gaussian processes in machine learning. In *Advanced lectures on machine learning*, pages 63–71. Springer, 2004.
- [26] Christian Robert. *The Bayesian choice: from decision-theoretic foundations to computational implementation*. Springer Science & Business Media, 2007.
- [27] Christian Robert and George Casella. Monte carlo statistical methods. *Springer, New York*, 2004.
- [28] Thomas Schreiber and Peter Grassberger. A simple noise-reduction method for real data. *Physics letters A*, 160(5):411–418, 1991.
- [29] Marek Strumik and Wiesław M Macek. Influence of dynamical noise on time series generated by nonlinear maps. *Physica D: Nonlinear Phenomena*, 237(5):613–618, 2008.
- [30] David M Walker and Alistair I Mees. Noise reduction of chaotic systems by kalman filtering and by shadowing. *International Journal of Bifurcation and Chaos*, 7(03):769–779, 1997.